

Contents

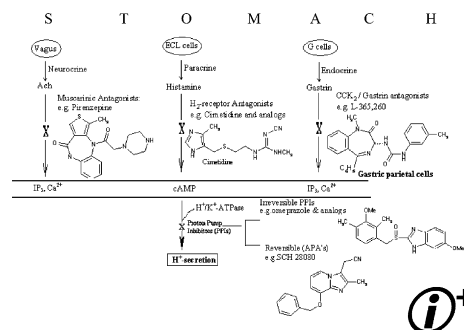
REVIEW

Recent advances in proton pump inhibitors and management of acid-peptic disorders

pp 1181–1205

Kishor S. Jain,* Anamik K. Shah, Jitender Bariwal, Suhas M. Shelke,
Amol P. Kale, Jayshree R. Jagtap and Ashok V. Bhosale

Ongoing research work on proton pump inhibitors has also been covered.

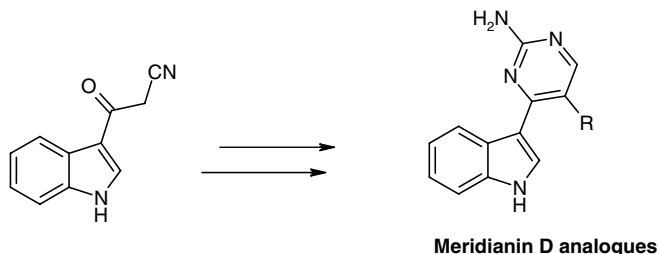


ARTICLES

Synthesis and antitumor activity of indolylpyrimidines: Marine natural product meridianin D analogues

pp 1206–1211

Mohamed A. A. Radwan* and Mahmoud El-Sherbiny

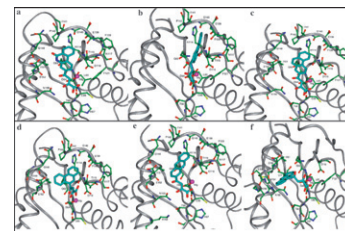


Synthesis and biological evaluation of novel 5(H)-phenanthridin-6-ones, 5(H)-phenanthridin-6-one diketo acid, and polycyclic aromatic diketo acid analogs as new HIV-1 integrase inhibitors

pp 1212–1228

Shivaputra Patil, Shantaram Kamath, Tino Sanchez, Nouri Neamati,*
Raymond F. Schinazi and John K. Buolamwini*

Substitution of β -diketo acid moiety onto the phenanthridinone and analogous polycyclic aromatic systems provided new potent HIV integrase (IN) inhibitors. The best IN inhibitor was, phenanthrene diketo acid, 2,4-dioxo-4-phenanthren-9-yl-butyric acid (**27f**), with an IC_{50} of 0.38 μ M against integrase strand transfer reaction. Compound **27d** had the best anti-viral activity against HIV replication in peripheral blood mononuclear cells, with an EC_{50} of 8.0 μ M and selectivity index of 10.

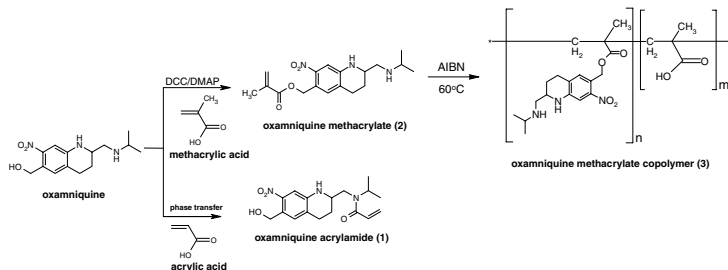


Design, synthesis, and in vivo evaluation of oxamniquine methacrylate and acrylamide prodrugs

pp 1229–1236

Roberto Parise Filho,* Carla Maria de Souza Menezes, Pedro Luiz Silva Pinto, Gilberto Alvarenga Paula, Carlos Alberto Brandt and Maria Amélia Barata da Silveira

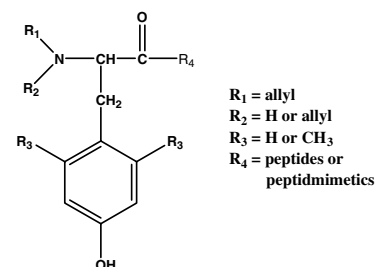
Starting from acrylic and methacrylic units, monomeric (derivatives **1** and **2**) and polymeric prodrugs (derivative **3**) of oxamniquine were designed with the purpose to prolong action. The compounds were tested in vivo and molecular modeling was applied to explain divergent results in oxamniquine's reactivity.

**Transformation of μ -opioid receptor agonists into biologically potent μ -opioid receptor antagonists**

pp 1237–1251

Tingyou Li, Yunden Jinsmaa, Masahiro Nedachi, Anna Miyazaki, Yuko Tsuda, Akihiro Ambo, Yusuke Sasaki, Sharon D. Bryant, Ewa Marczak, Qiang Li, H. Scott Swartzwelder, Lawrence H. Lazarus* and Yoshio Okada*

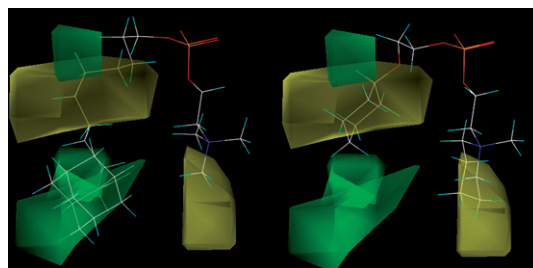
A series of potent μ -opioid receptor-selective antagonists were developed and their biological activities in vitro and in vivo are reported.

**3D-Quantitative structure–activity relationships of synthetic antileishmanial ring-substituted ether phospholipids**

pp 1252–1265

Agnes Kapou, Nikolas P. Benetis, Nikos Avlonitis, Theodora Calogeropoulou, Maria Koufaki, Efi Scoullica, Sotiris S. Nikolaropoulos and Thomas Mavromoustakos*

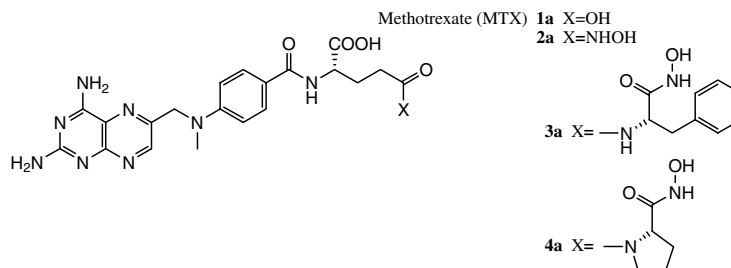
The correlation of the in vitro antileishmanial activity against the promastigote forms of *Leishmania infantum* and *Leishmania donovani* for a series of 33 flexible synthetic 2-(4-alkylidene-cyclohexyloxy)ethyl- or ω -cycloalkylidene-substituted ether phospholipids with their 3D structure was systematically evaluated by CoMFA and CoMSIA 3D-QSAR studies.

**Methotrexate γ -hydroxamate derivatives as potential dual target antitumor drugs**

pp 1266–1274

M. Amélia Santos,* Eva A. Enyedy, Elisa Nuti, Armando Rossello, Natalia I. Krupenko and Sergey A. Krupenko

A series of new aminopteroyl-based hydroxamate derivatives was synthesized and tested in vitro in cell culture models and as inhibitors of two families of enzymes, matrix metalloproteinases (MMP) and dihydrofolate reductase (DHFR), which are the components of two unrelated cellular pathways in metastasizing tumors.



pp 1275–1279

pp 1280–1288

Chemical structures of three quinoline derivatives:

- Structure 1: 6,8-dinitro-2-hydroxy-3-phenylquinoline (R = phenyl)
- Structure 2: 6,8-diamino-2-hydroxy-3-phenylquinoline (R = phenyl)
- Structure 3: General quinoline derivative with substituents R' and R, and a bridgehead X (X = C or N)

$[^{11}\text{C}]\text{HC-15 } ([^{11}\text{C}]\text{1})$

$[^{18}\text{F}]\text{HC-15 } ([^{18}\text{F}]\text{2})$

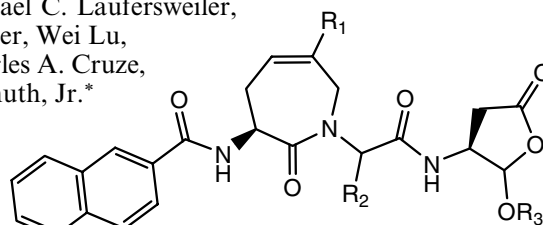
pp 1298–1310

Synthesis and evaluation of unsaturated caprolactams as interleukin-1 β converting enzyme (ICE) inhibitors

pp 1311–1322

Yili Wang, Steven V. O'Neil, John A. Wos,* Kofi A. Oppong, Michael C. Lauferweiler, David L. Soper, Christopher D. Ellis, Mark W. Baize, Amy N. Fancher, Wei Lu, Maureen K. Suchanek, Richard L. Wang, William P. Schwecke, Charles A. Cruze, Maria Buchalova, Marina Belkin, Biswanath De and Thomas P. Demuth, Jr.*

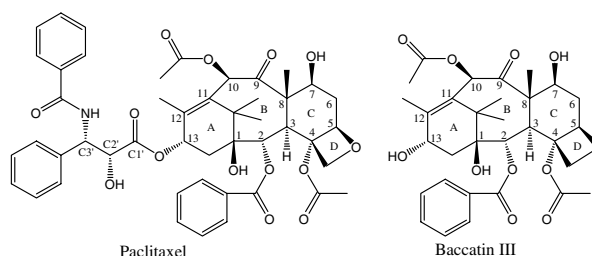
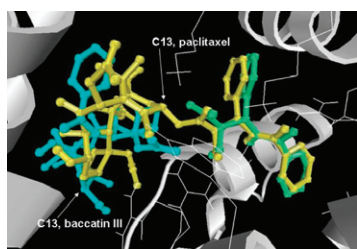
Peptidomimetic compounds possessing a caprolactam ring constraint were prepared as interleukin-1 β converting enzyme (ICE) inhibitors. Several compounds exhibited significant potency in vitro (<10 nM) and excellent bioavailability ($F > 50\%$) in rats.



Paclitaxel binding to human serum albumin—Automated docking studies

pp 1323–1329

Krisztina Paal,* Aliaksei Shkarupin and Laura Beckford

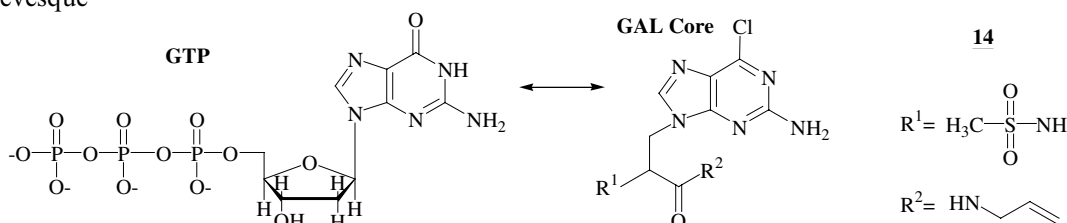


The paclitaxel binding sites on human serum albumin have been located by automated docking. The binding mode at the primary site appears to be governed by the C13 side chain.

Parallel solid synthesis of inhibitors of the essential cell division FtsZ enzyme as a new potential class of antibacterials

pp 1330–1340

Catherine Paradis-Bleau, Mélanie Beaumont, François Sanschagrin, Normand Voyer and Roger C. Levesque*

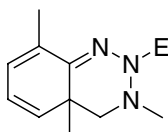


GTP analogues were synthesized with a guanine-like moiety linked to an Ala side chain using combinatorial chemistry as FtsZ GTPase inhibitors. Lead compound **14** showed prominent inhibitory and antibacterial activities.

Tetrahydrobenzotriazines as a new class of nematocide

pp 1341–1345

Keiji Nishiwaki,* Azusa Okamoto, Keizo Matsuo,* Yoshio Hayase, Shunichiro Masaki, Riichi Hasegawa and Katsuaki Ohba

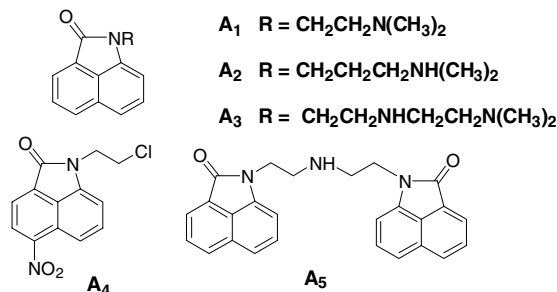


E = acetyl, COR, CONHPh, etc.

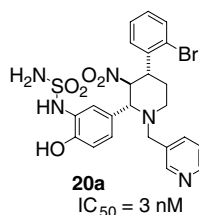
pp 1346–1355

OC(=O)CC[C@H](O)[C@H](O)C(=O)O
 $\xrightarrow[\text{NAD}^+ \rightarrow \text{NADH}]{\text{homoisocitrate dehydrogenase (HICDH)}}$
OC(=O)CC[C@H](C(=O)O)C(=O)O
 $\xrightarrow{-\text{CO}_2}$
OC(=O)CC[C@H](C(=O)O)C(=O)O

Hong Yin, Yufang Xu and Xuhong Qian*

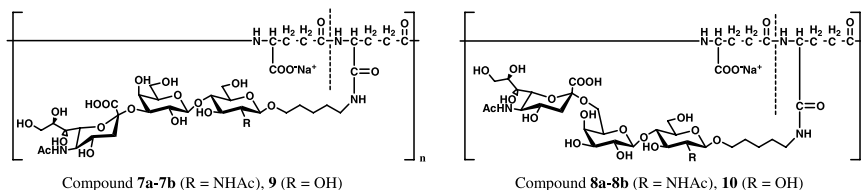


Rieko Tanaka, Almudena Rubio, Nancy K. Harn, Douglas Gernert, Timothy A. Grese, Jun Eishima, Mitsunobu Hara, Nobuyuki Yoda, Rui Ohashi, Takashi Kuwabara, Shiro Soga, Shiro Akinaga, Shinji Nara and Yutaka Kanda*



Metabolically stable compound **20a** with potent FTase inhibition ($IC_{50} = 3$ nM) is reported.

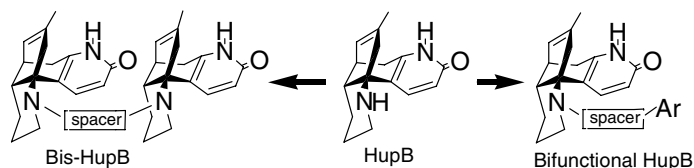
Makoto Ogata, Takeomi Murata, Kouki Murakami, Takashi Suzuki, Kazuya I. P. J. Hidari,
Yasuo Suzuki and Taichi Usui*



A novel synthetic method of artificial glycopolypeptides was reported. The avian influenza virus bound strongly to Neu5Ac α 2,3LacNAc/Lac-carrying glycopolypeptides, whereas the human influenza virus bound to Neu5Ac α 2,6LacNAc in preference to Neu5Ac α 2,6Lac.

Study on dual-site inhibitors of acetylcholinesterase: Highly potent derivatives of bis- and bifunctional huperzine B pp 1394–1408

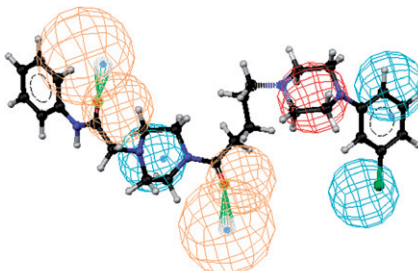
Xu-Chang He,* Song Feng, Zhi-Fei Wang, Yufang Shi, Suxin Zheng, Yu Xia, Hualiang Jiang, Xi-Can Tang and Donglu Bai



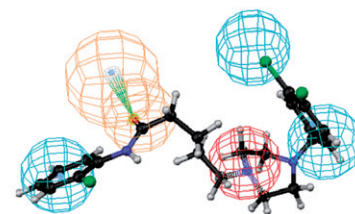
Lead discovery and optimization of T-type calcium channel blockers pp 1409–1419

Jung Hwan Park, Jin Kyu Choi, Eunjung Lee, Jae Kyun Lee, Hyewhon Rhim, Seon Hee Seo, Yoonjee Kim, Munikumar Reddy Doddareddy, Ae Nim Pae, Jahyo Kang and Eun Joo Roh*

Novel series of piperazine derivatives with hypothetical pharmacophoric features were prepared and evaluated for T-type calcium channel (α_1G) by FDSS assay and patch clamp method. Among them, alkanamide derivatives with 4-arylsubstituted piperazine (**7b**, **9j**, **11b**, **11g**, **11h**) showed better efficacy than Mibefradil.



Mapping of **5a** with 6 feature hypothesis

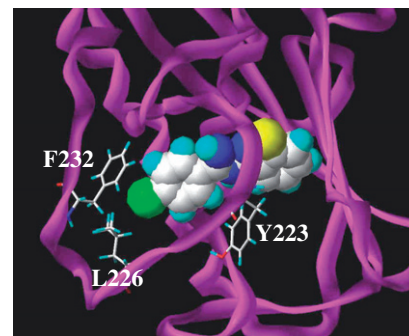


Mapping of **11g** with 5 feature hypothesis

Molecular modeling of binding between amidinobenzisothiazoles, with antidegenerative activity on cartilage, and matrix metalloproteinase-3 pp 1420–1429

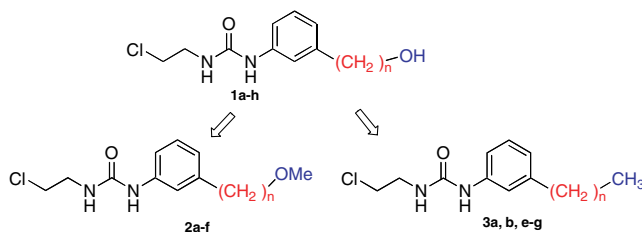
Alessio Amadasi, Pietro Cozzini,* Matteo Incerti, Elenia Duce, Emilia Fisicaro and Paola Vicini

N-(Benzo[*d*]isothiazol-3-yl)-4-chlorobenzamidine bound within the binding site of MMP-3, as predicted by molecular docking calculations using the published 1CIZ X-ray structure.



N-Phenyl-*N'*-(2-chloroethyl)ureas (CEU) as potential antineoplastic agents. Part 2: Role of ω -hydroxyl group in the covalent binding to β -tubulin pp 1430–1438

Sébastien Fortin, Emmanuel Moreau,* Alexandre Patenaude, Michel Desjardins, Jacques Lacroix, Jean L. C. Rousseau and René C-Gaudreault*

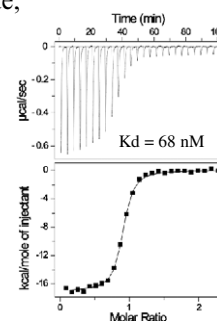
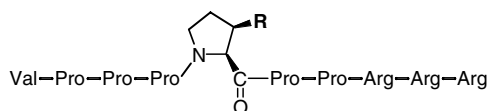


Importance of chain length and ω -hydroxyl group on cell growth inhibition and β -tubulin alkylation.

High affinity Grb2-SH3 domain ligand incorporating C β -substituted prolines in a Sos-derived decapeptide

pp 1439–1447

Yves Jacquot,* Isabelle Broutin, Emeric Miclet, Magali Nicaise, Olivier Lequin, Nicole Goasdoué, Charlotte Joss, Philippe Karoyan, Michel Desmadril, Arnaud Ducruix and Solange Lavielle

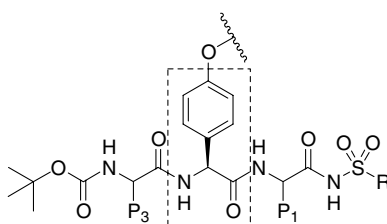


Sos-derived decapeptides incorporating C β -substituted prolines were synthesized and evaluated for their ability to bind recombinant Grb2. Affinities were increased up to 560 times compared to the wild-type peptide.

Phenylglycine as a novel P2 scaffold in hepatitis C virus NS3 protease inhibitors

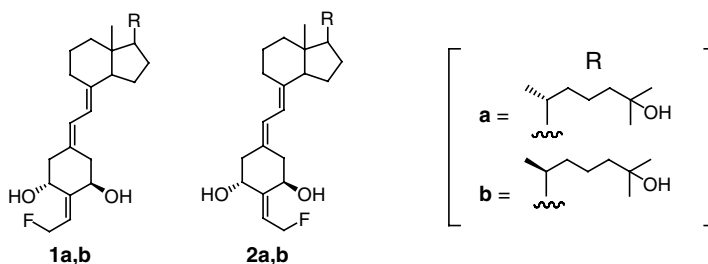
pp 1448–1474

Pernilla Örtqvist, Shane D. Peterson, Eva Åkerblom, Thomas Gossas, Yogesh A. Sabnis, Rebecca Fransson, Gunnar Lindeberg, U. Helena Danielson, Anders Karlén and Anja Sandström*

**Structure–activity relationships of 19-norvitamin D analogs having a fluoroethylidene group at the C-2 position**

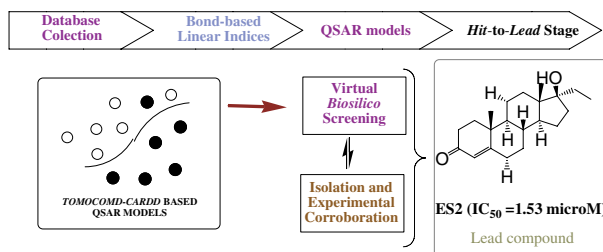
pp 1475–1482

Emi Kobayashi, Mika Shimazaki, Yukiko Miyamoto, Hiroyuki Masuno, Keiko Yamamoto, Hector F. DeLuca, Sachiko Yamada and Masato Shimizu*

**TOMOCOMD-CARDD descriptors-based virtual screening of tyrosinase inhibitors: Evaluation of different classification model combinations using bond-based linear indices**

pp 1483–1503

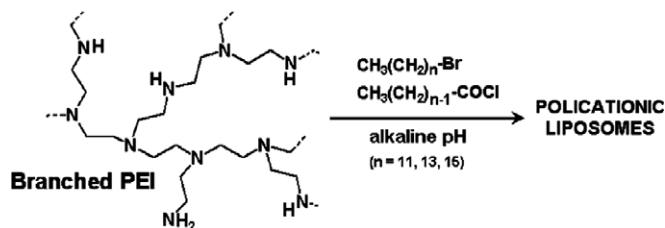
Gerardo M. Casañola-Martín, Yovani Marrero-Ponce,* Mahmud Tareq Hassan Khan, Arjumand Ather, Sadia Sultan, Francisco Torrens and Richard Rotondo



Physicochemical and biological study of selected hydrophobic polyethylenimine-based polycationic liposomes and their complexes with DNA

pp 1504–1515

Andrea Masotti,* Fabiola Moretti, Francesca Mancini, Giuseppina Russo, Nicoletta Di Lauro, Paola Checchia, Carlotta Marianecchi, Maria Carafa, Eleonora Santucci and Giancarlo Ortaggi



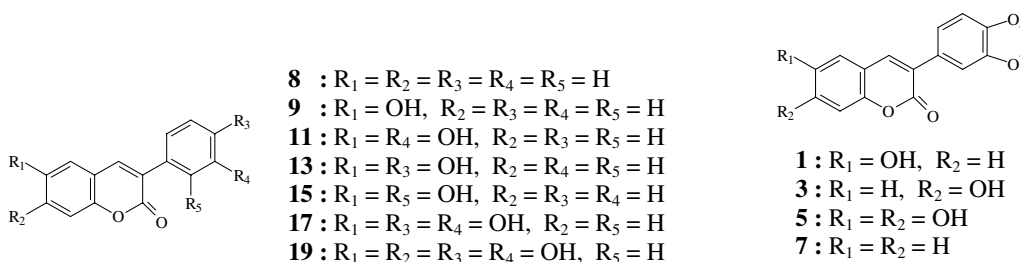
Hydrophobic PEI's derivatives display low toxicities in vitro, and are able to compact DNA in small and stable complexes.

Inhibition of horseradish peroxidase catalytic activity by new 3-phenylcoumarin derivatives:

pp 1516–1524

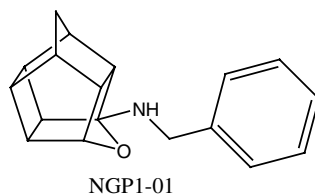
Synthesis and structure–activity relationships

Luciana M. Kabeya, Anderson A. de Marchi, Alexandre Kanashiro, Norberto P. Lopes, Carlos H. T. P. da Silva, Mônica T. Pupo* and Yara M. Lucisano-Valim*


Structure–activity relationships of pentacycloundecylamines at the *N*-methyl-D-aspartate receptor

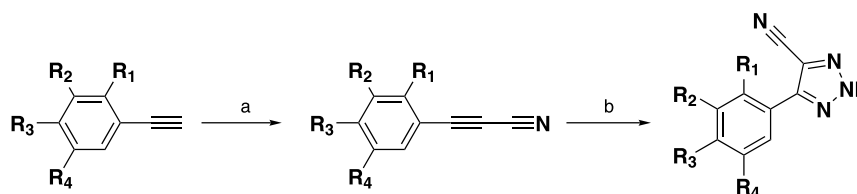
pp 1525–1532

Werner J. Geldenhuys, Sarel F. Malan, Jeffrey R. Bloomquist and Cornelis J. Van der Schyf*


Synthesis and biological evaluation of 4-aryl-5-cyano-2*H*-1,2,3-triazoles as inhibitor of HER2 tyrosine kinase

pp 1533–1538

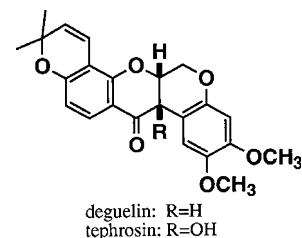
Zhi-Yi Cheng,* Wen-Jie Li, Feng He, Jun-Min Zhou and Xiao-Feng Zhu*



(a) CuCN, $(\text{CH}_3)_3\text{SiCl}$, NaI(Cat.); DMSO/ $\text{CH}_3\text{CN}/\text{H}_2\text{O}$, 50 °C, 24–72 h (b) NaN_3 , 90–120 °C, 1.5 h.

pp 1539–1546

Principal rotenoids (deguelin, tephrosin, rotenone, and 12a-hydroxyrotenone) (3–30 μ M) isolated from the stems of *Erycibe expansa* significantly inhibited invasion of human fibrosarcoma HT1080 cells through Matrigel-coated filters and release of proMMPs-2 and 9. In addition, deguelin and tephrosin showed differentiation-inducing activity in human promyelocytic leukemia HL-60 cells. Furthermore, effects of various constituents isolated from the ethyl acetate-soluble fraction on proliferation of human leukemia U937 cells were examined. As a result, most of isoflavones and several flavans as well as rotenoids showed moderate or substantial anti-proliferative activities.



pp 1547–1555

Chemical reaction scheme showing the synthesis of a chiral amine derivative. The starting material is (S)-1-(4-hydroxybenzyl)propan-2-amine methyl ester. It reacts with a chiral auxiliary, (S)-1-(4-hydroxybenzyl)-2-methyl-3-oxo-3-phenylbutan-1-amine methyl ester, to form a chiral amine derivative. The auxiliary is then removed using HET (hydroxyethyltrimethylsilyl) to yield the final product, (S)-1-(4-(2-(hydroxyethyl)oxyphenyl)benzyl)propan-2-amine methyl ester.

pp 1556–1567

Diagram illustrating a 3D helical structure. The distance d is given as $d = 5 - 5.5 \text{ \AA}$. The bond angles are labeled as $\tau_4 = 0^\circ$, $\tau_1 = -64^\circ$, $\tau_2 = -152^\circ$, and $\tau_3 = -180^\circ$. A cluster of green dots is shown at the bottom left.


Proposed pharmacophore for anticonvulsant activity, derived from a CoMFA that uses a training set of 27 AC drugs. New AC symmetric sulfamides were designed on its basis.

pp 1568–1571

[illegible]

OTHER CONTENTS**Corrigendum****p 1572****Bioorganic & Medicinal Chemistry Reviews and Perspectives****pp 1573–1575****Summary of instructions to authors****p I**

*Corresponding author

 * Supplementary data available via ScienceDirect**COVER**

Terfenadine (an antihistamine pulled from the market in 1997) bound to a model of an open form of the homo-tetrameric pore domain of hERG, produced using Schrödinger's "Induced Fit Docking" technology [Farid, R.; Day, T.; Friesner, R. A.; Pearlstein, R. A. *Bioorg. Med. Chem.* **2006**, *14*, 3160–3173].

Available online at

www.sciencedirect.com

Indexed/Abstracted in: Beilstein, Biochemistry & Biophysics Citation Index, CANCERLIT, Chemical Abstracts, Chemistry Citation Index, Current Awareness in Biological Sciences/BIODISE, Current Contents: Life Sciences, EMBASE/Excerpta Medica, MEDLINE, PASCAL, Research Alert, Science Citation Index, SciSearch, TOXFILE

**ELSEVIER**

ISSN 0968-0896